Synthesis of anion M-doped NiCoP (M = S, Se and N) as bifunctional catalysts for alkaline seawater and urea splitting

Han Zhao[a], Min Liu[a], Xiaoqiang Du[a*]and Xiaoshuang Zhang[b]

[a] School of Chemistry and Chemical Engineering , Shanxi Key Laboratory of High Performance Battery Materials and Devices, North University of China, Xueyuan road 3, Taiyuan 030051, People's Republic of China. E-mail: duxq16@nuc.edu.cn

[b] School of Environment and Safety Engineering, North University of China, Xueyuan road 3, Taiyuan 030051, People's Republic of China.

Chemicals and reagents

Nickel foam (NF, thickness 1.0 mm) was purchased from Kunshan Guangjiayu New Material Co., Ltd; Sublimation sulphur was purchased from Tianjin Windship Chemical Reagent Technology Co., Ltd; Selenium powder was purchased from Aiwan (Shanghai) Chemical Technology Co., Ltd; Sodium hypophosphite monohydrate ($NaPO_2H_2·H_2O$) was purchased from Shanghai Aladdin Biochemical Technology Co., Ltd; Ammonium fluoride (NH_4F) was purchased from Sinopharm Chemical Reagent Co., Ltd; Potassium hydroxide (KOH), hexahydrate ($Co(NO_3)_2·6H_2O$), Nickel nitrate hexahydrate ($Ni(NO_3)_2·6H_2O$), urea ($CO(NH_2)_2$) were purchased from Tianjin Damao Chemical Reagent Factory; Concentrated hydrochloric acid (HCl, 12 mol/L) was purchased from Chengdu Colon Chemical Co., Ltd.

Material characterization

The morphology of the catalyst was characterized by scanning electron microscopy (SEM) and HITACHI SU8000. Transmission electron microscopy (TEM TECNAI G2) was used to observe the microstructure and lattice fringes of the electrodes, and to characterize the spatial distribution of elements. The electrode composition and purity were researched by X-ray powder diffraction (XRD, Rigaku, Cu Ka radiation, k =1.5406A). The surface properties and oxidation states of the electrodes were researched by X-ray photoelectron spectroscopy (XPS, Axi-Ultra ddd-600 W), and the C1s peaks of each material were calibrated with reference values of 284.6 eV.

Electrochemical test

Electrocatalytic data were researched at the CHI760e electrochemical workstation. Electrochemical tests were carried out in a standard three-electrode system, with Hg/HgO

electrode as the reference electrode, graphite rod as the counter electrode, and the prepared synthetic material as the working electrode. All measurements were performed in an alkaline medium for HER (1.0 M KOH+Seawater) and (1.0 M KOH + 0.5 M Urea)，UOR (1.0 M KOH + 0.5 M Urea). The potential involved is converted based on the following formula: E (RHE) = E (Hg/HgO) +0.098 +0.059* pH (1 M KOH, pH = 13.6). Linear sweep voltammetry (LSV) was obtained to research the performance of the electrode. Cyclic voltammetry (CV) curves are also tested at different sweep speeds in the nonFaraday region to assess the double layer capacitance of the electrode, which can reflect the size of the electrochemically surface area (ECSA) of the electrode. The electrochemical active surface area (ECSA) was calculated from the double-layer capacitance (C_{dl}) by the equation of ECSA = S × C_{dl}/C_s (in alkaline solution containing 1.0 M KOH, S is the working electrode area, C_s=0.04 mF cm^{-2}). Electrochemical impedance spectroscopy (EIS) was performed at a constant voltage in frequency range between $1*10^{-2}$ Hz and $1*10^{5}$ Hz, and the test voltage for the EIS is set to -1.25 V. All electrocatalytic measurements were performed under compensated conditions (iR =70%).

DFT computation details:

The DFT calculations were performed using the Cambridge Sequential Total Energy Package (CASTEP) with the plane-wave pseudo-potential method. The geometrical structures of the (100) plane of NiCoP was optimized by the generalized gradient approximation (GGA) methods. The Revised Perdew-Burke-Ernzerh of (RPBE) functional was used to treat the electron exchange correlation interactions. A Monkhorst Pack grid k-point of 3*5*1 of NiCoP ,a plane-wave basis set cut-off energy of 400 eV were used for integration of the Brillouin zone. The structures were optimized for energy and force convergence set at 0.05 eV/A and 2.0×10^{-5} eV, respectively. The Gibbs free energy of H adsorption was calculated as follows:

$\Delta G_{H^*} = \Delta E_{H^*} + \Delta ZPE - T\Delta S$

Where ΔZPE is the zero-point energy and TΔS stands for the entropy corrections. According to the previous report by Norskov et al., we used the 0.24 eV for the ΔZPE - TΔS of hydrogen adsorption in this work.

Res: J. Electrochem. Soc., **2005**, 152, J23.

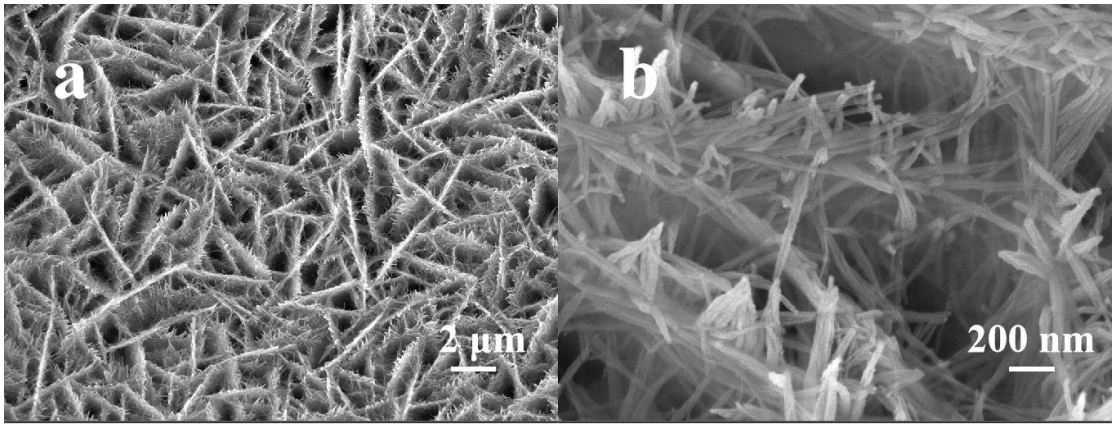

Fig.S1 SEM images of $Co(OH)_2$/NF.

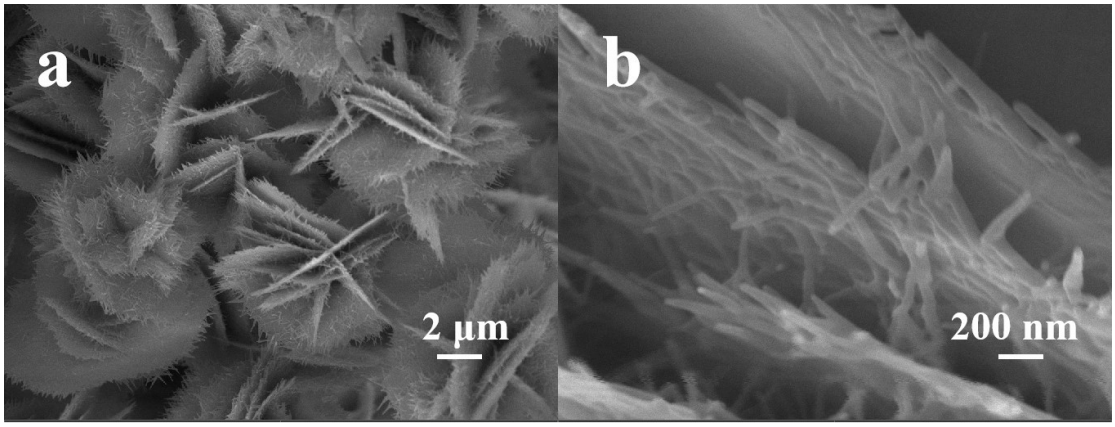

Fig.S2 SEM images of NiCoP.

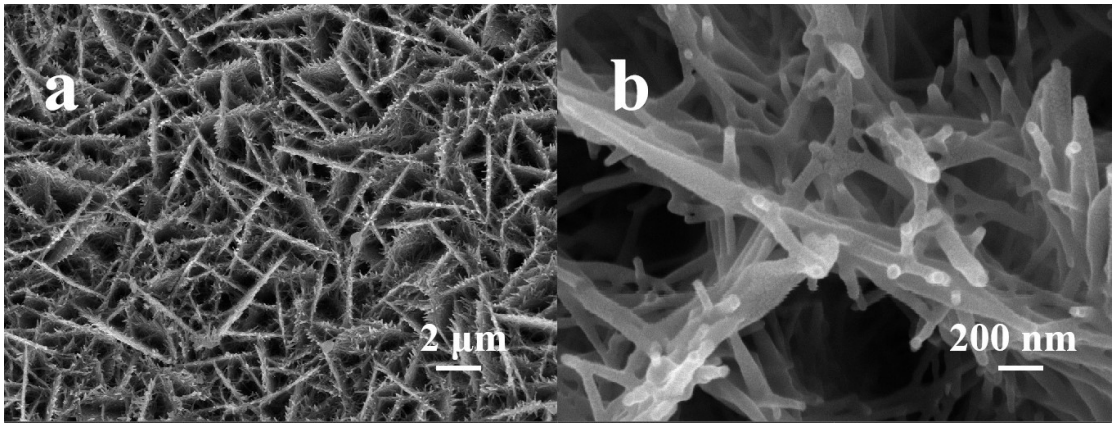

Fig.S3 SEM images of NiCoP-Se.

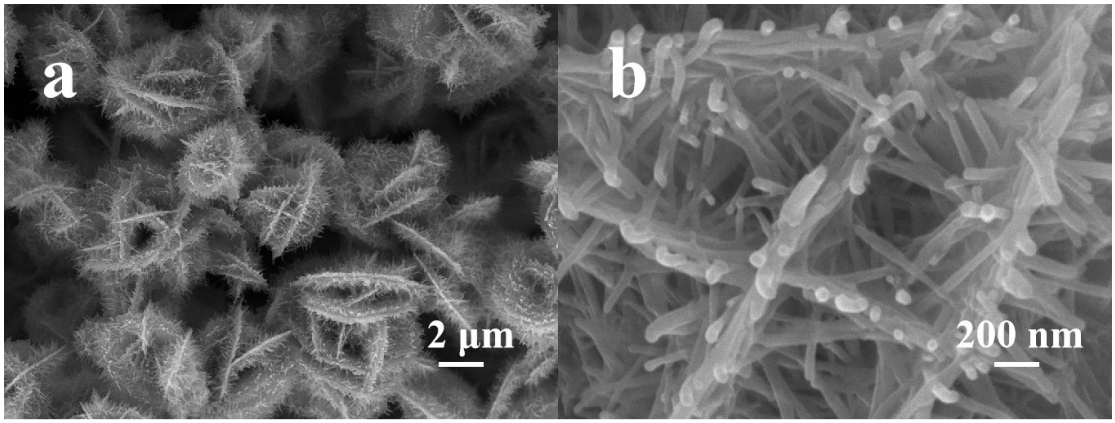

Fig.S4 SEM images of NiCoP-N.

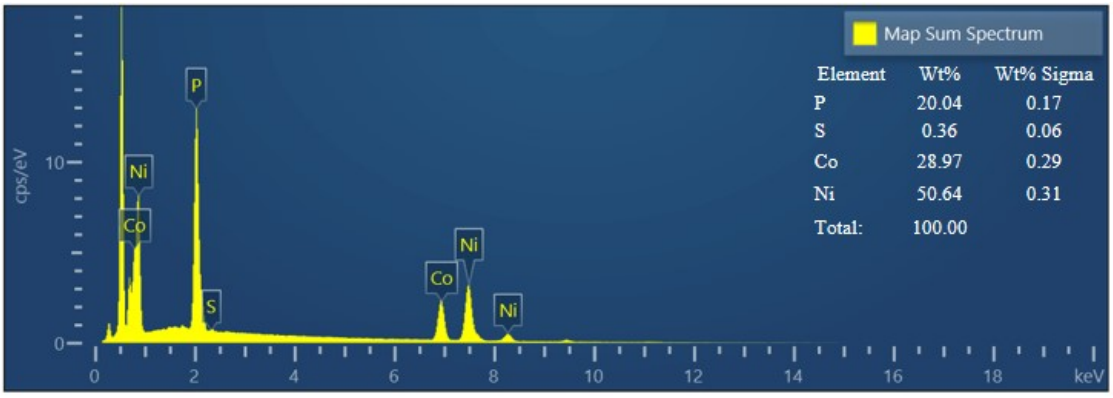

Fig.S5 EDS spectrum of NiCoP-S and corresponding element atomic percentage.

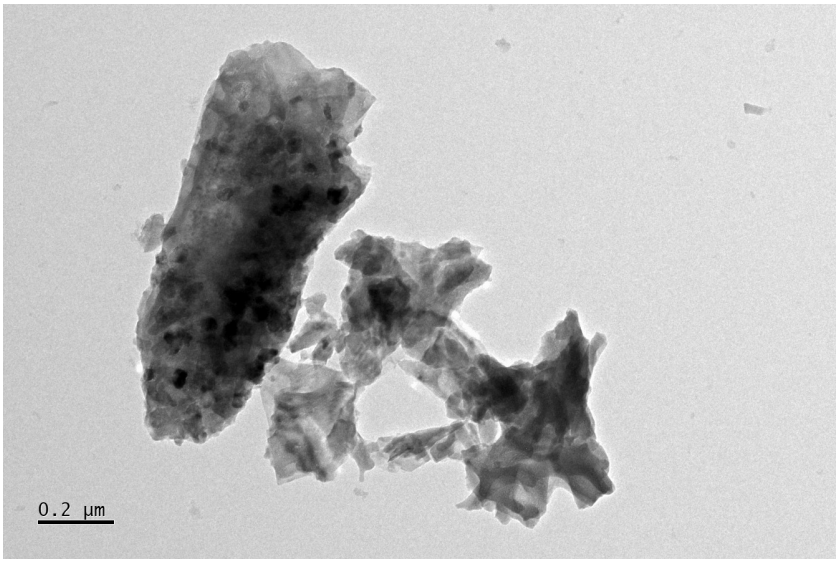

Fig.S6 TEM images of NiCoP-S.

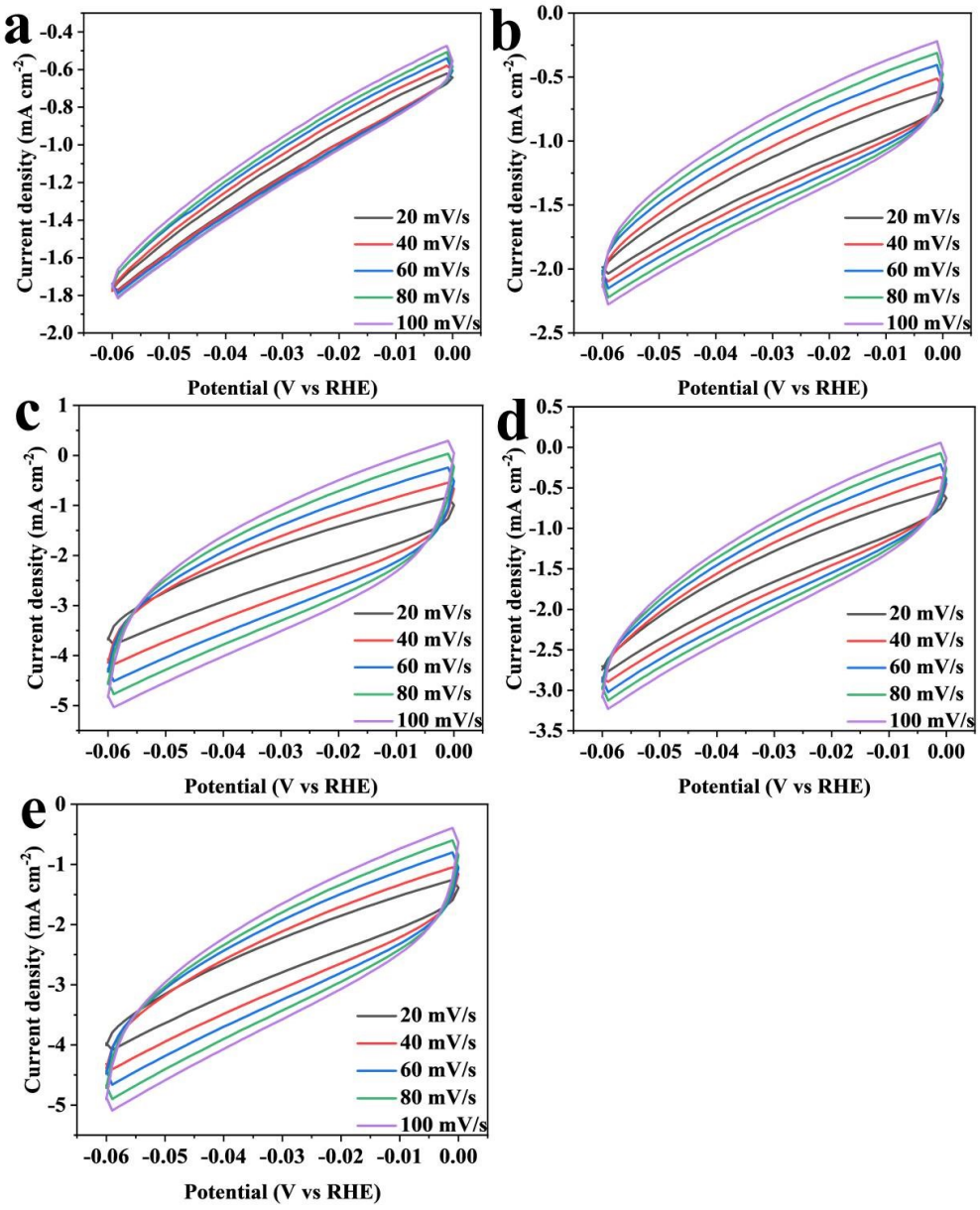

Fig.S7 CV plots of a) $Co(OH)_2$/NF, b) NiCoP, c) NiCoP-S, d) NiCoP-Se, e) NiCoP-N at different scan rates of HER in 1.0 M KOH + 0.5 M Urea.

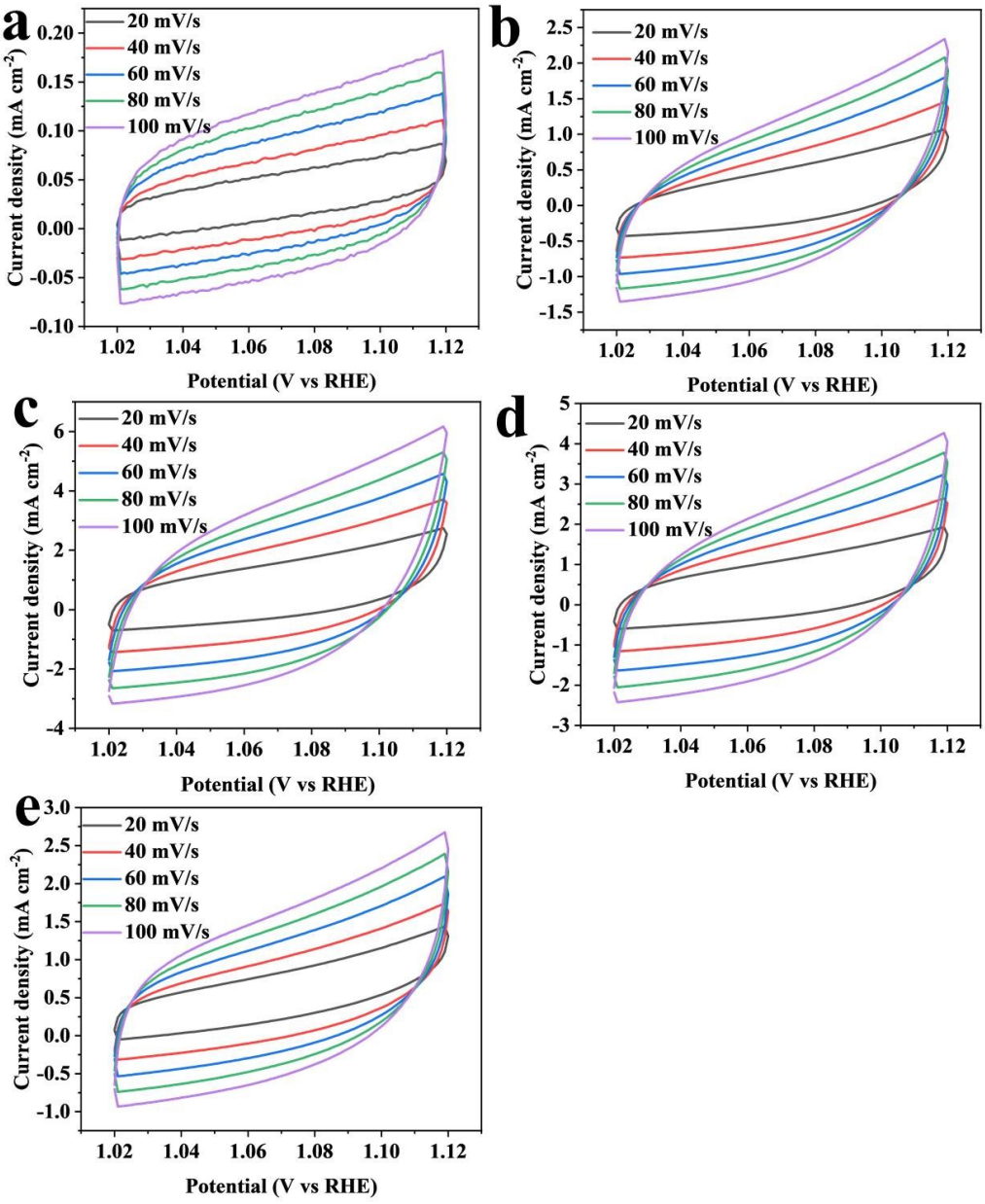

Fig.S8 CV plots of a) $Co(OH)_2$/NF, b) NiCoP, c) NiCoP-S, d) NiCoP-Se, e) NiCoP-N at different scan rates of UOR in 1.0 M KOH + 0.5 M Urea.

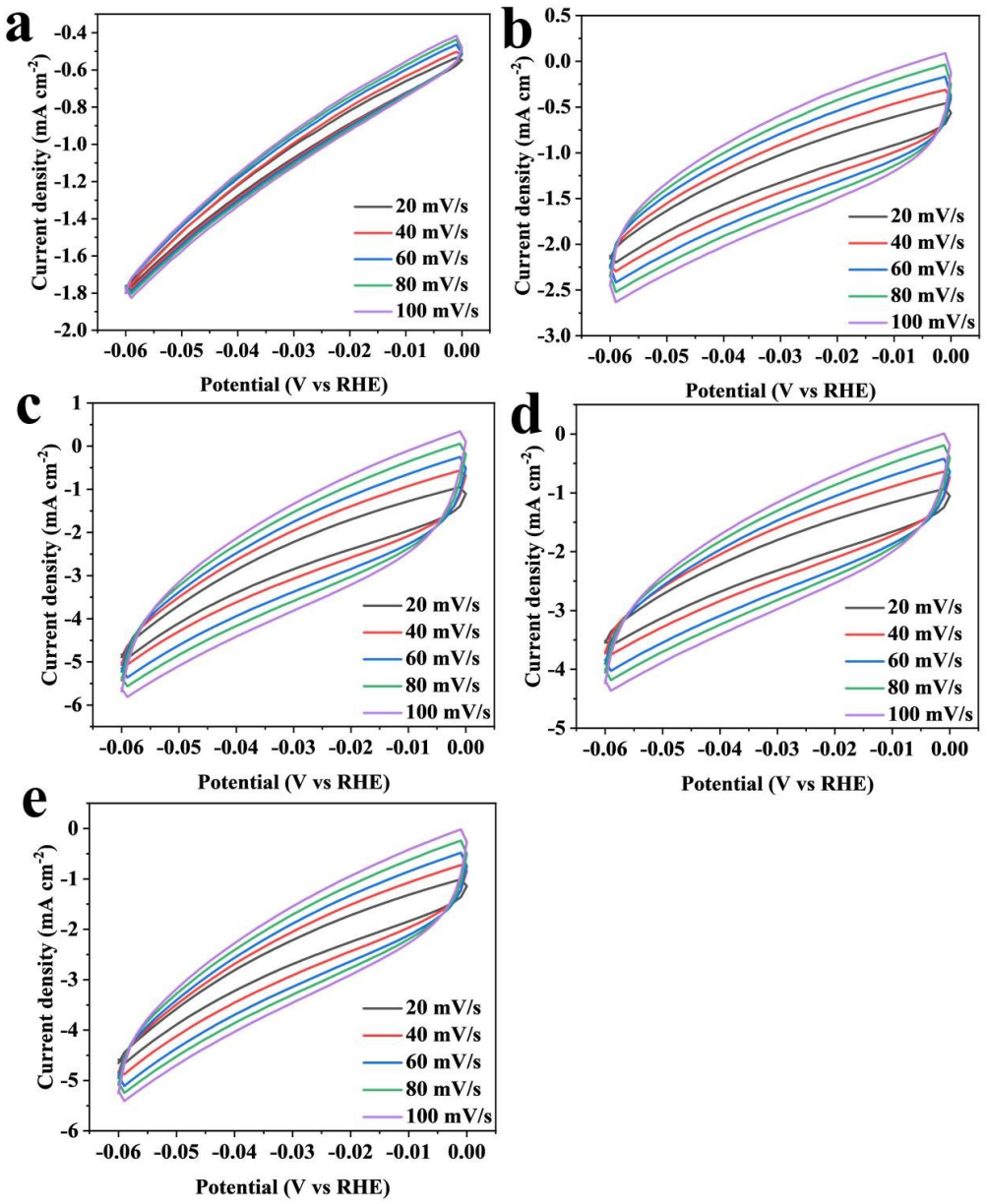

Fig.S9 CV plots of a) $Co(OH)_2$/NF, b) NiCoP, c) NiCoP-S, d) NiCoP-Se, e) NiCoP-N at different scan rates of HER in 1.0 M KOH+Seawater.

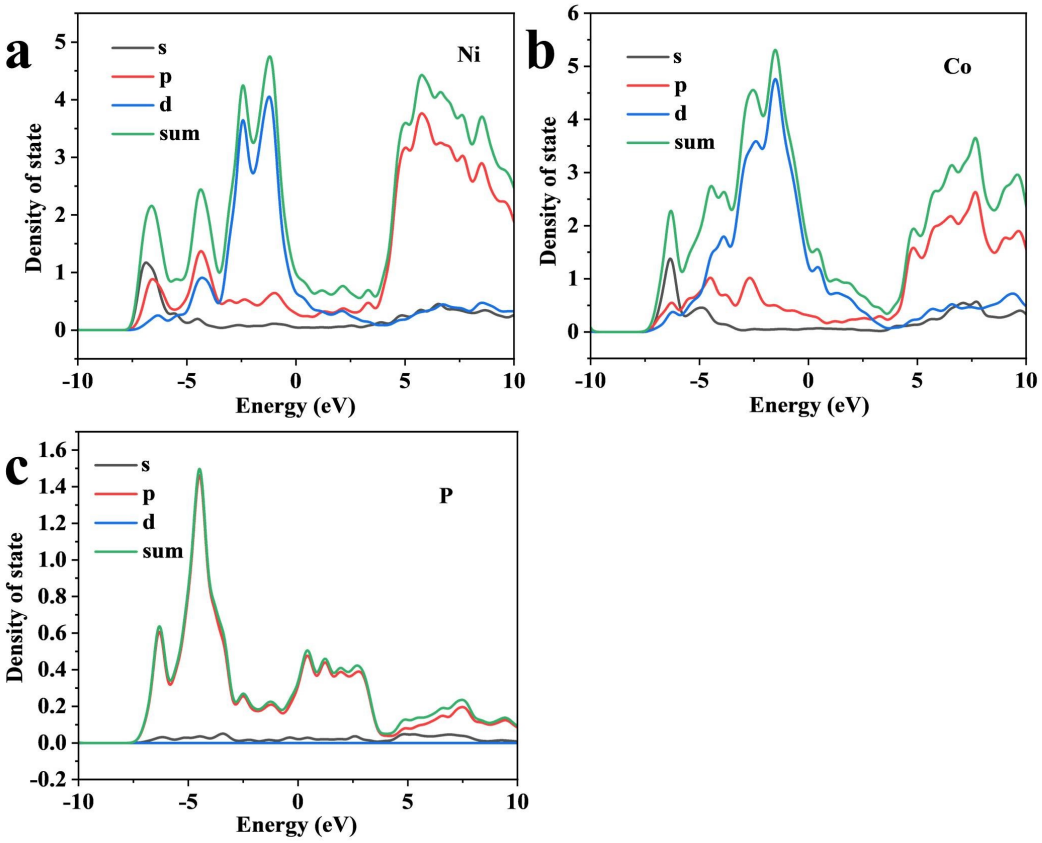

Fig. S10 Density of states for NiCoP, (a) Ni, (b) Co and (c) P.

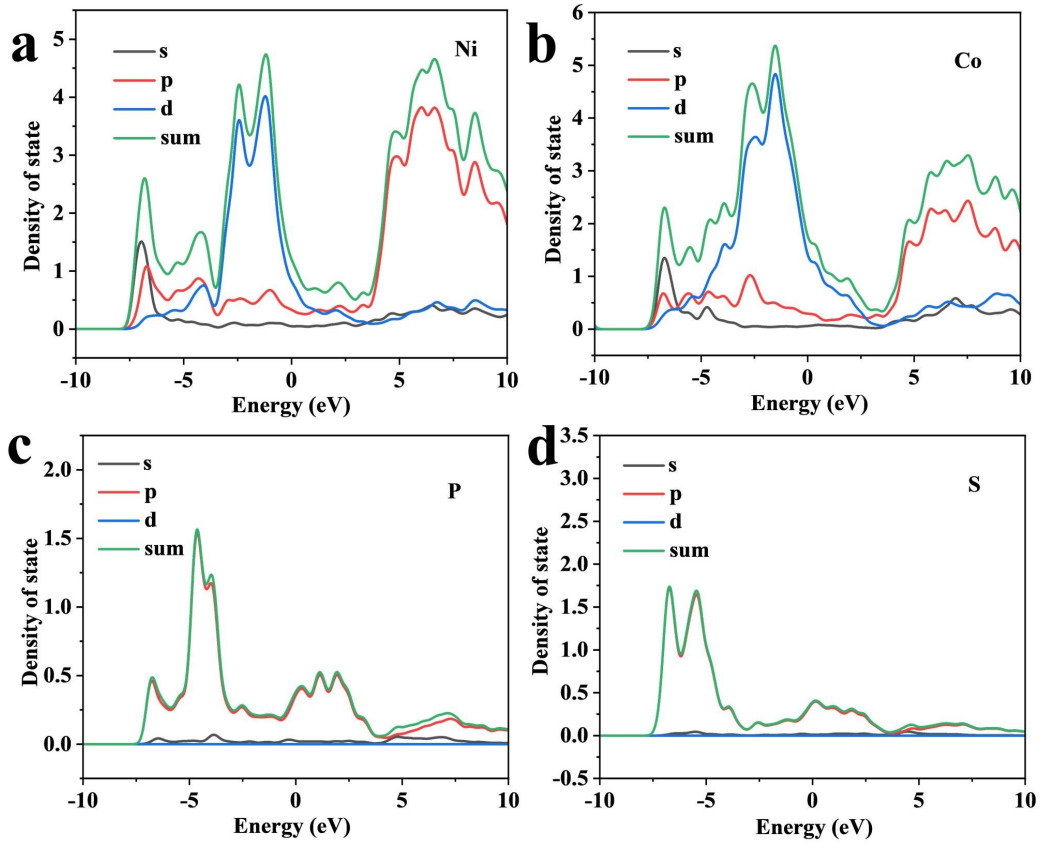

Fig. S11 Density of states for NiCoP-S, (a) Ni, (b) Co, (c) P and (d) S.

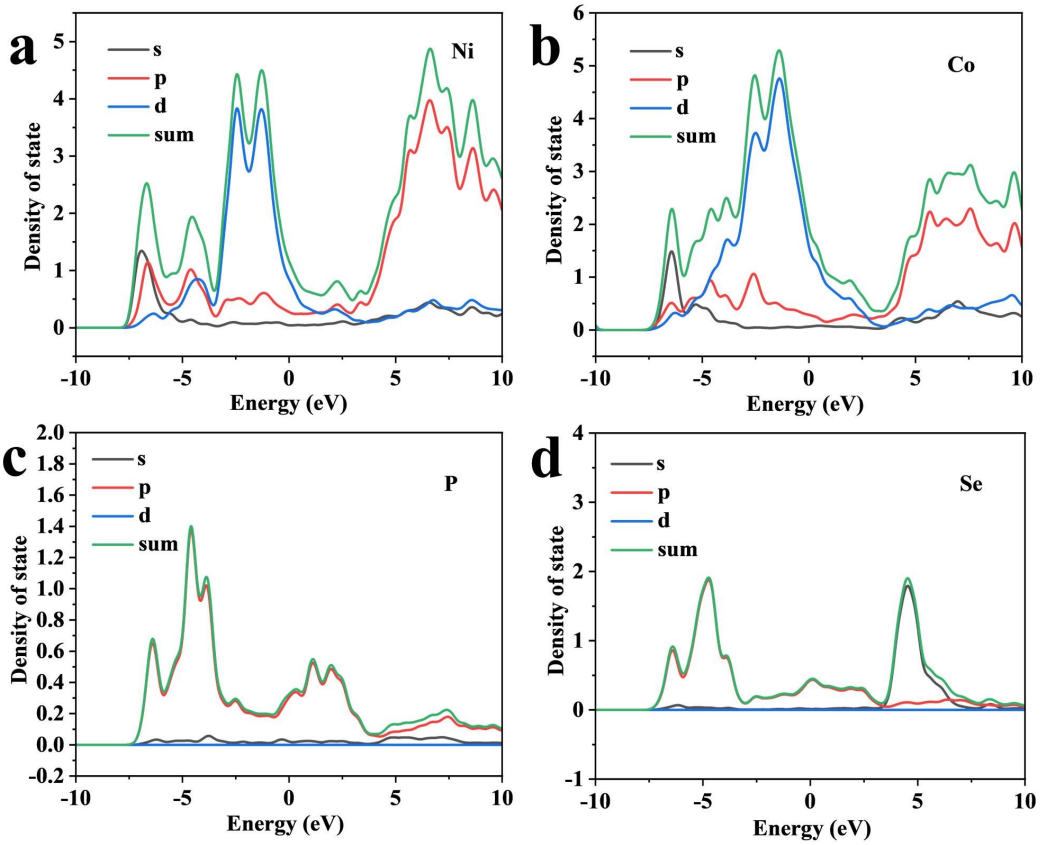

Fig. S12 Density of states for NiCoP-Se, (a) Ni, (b) Co, (c) P and (d) Se.

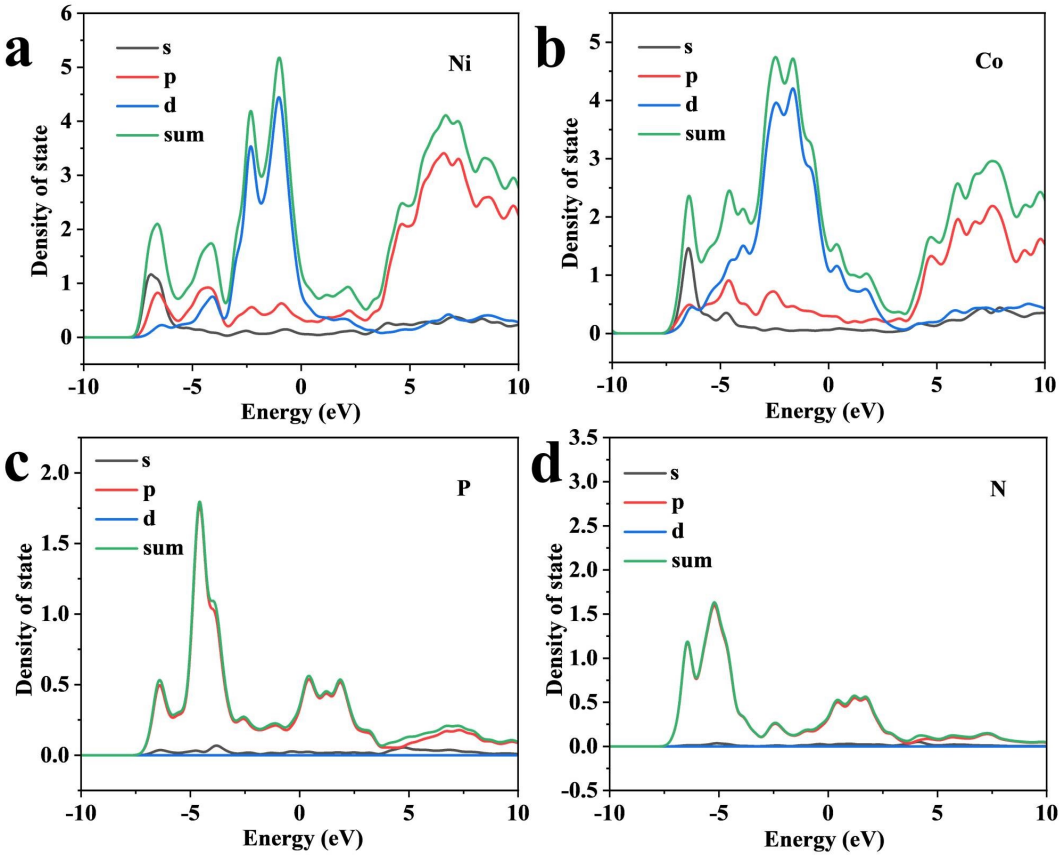

Fig. S13 Density of states for NiCoP-N, (a) Ni, (b) Co, (c) P and (d) N.

Table S1 Comparison of the HER performances of NiCoP-S and other reported electrocatalysts in alkaline solutions containing urea.

catalysts	Electrolytes	pH	Overpotential(V) at 100 mA/cm^2	Reference
NiCoP-S	**1M KOH + 0.5 Urea**	**13.6**	**170 mV**	**This work**
Ni_3N/NF	1M KOH + 0.5 Urea	14	287 mV	[1]
Fe_2P@Ni_xP/NF	1M KOH + 0.5 Urea	14	219 mV	[2]
CoMn/$CoMn_2O_4$	1M KOH + 0.5 Urea	14	165 mV	[3]
NF/CoP@Ni_3S_2	1M KOH + 0.5 Urea	14	231 mV	[4]
Cu-Ni_3S_2@NiFe LDH	1M KOH + 0.5 Urea	14	223 mV	[5]
NiMo@ZnO/NF	1M KOH + 0.33 Urea	14	243 mV	[6]
Cu_2S@Ni_3Se_2	1M KOH + 0.5 Urea	14	199 mV	[7]
Ni_3S_2-NiS/NF	1M KOH + 0.5 Urea	14	301 mV	[8]
Fe-NiS-NiS_2	1M KOH + 0.5 Urea	14	267 mV	[9]
$Ni(OH)_x$/p-N	1M KOH + 0.33 Urea	14	220 mV	[10]

Table S2 Comparison of the UOR performances of NiCoP-S and other reported electrocatalysts in alkaline solutions containing urea.

catalysts	Electrolytes	pH	Potential(V) at 100 mA/cm^2	Reference
NiCoP-S	**1M KOH + 0.5M Urea**	**13.6**	**1.451 V**	**This work**
NiCoP	1M KOH + 0.5M Urea	14	1.55 V	[11]
a-FeCoO	1M KOH + 0.5M Urea	14	1.52 V	[12]
FeCoNiRu/CNFs	1M KOH + 0.33M Urea	14	1.49 V	[13]
CoS_2/MoS_2@FCP	1M KOH + 0.4M Urea	14	1.75 V	[14]
Fe–Ni_2P/$NiSe_2$-0	1M KOH + 0.33M Urea	14	1.455 V	[15]
$CoMoO_4$/NF	1M KOH + 0.33M Urea	14	1.695 V	[16]

CoS_2/Ni_3S_2/NF	1M KOH + 0.5M Urea	14	1.59 V	[17]
$Ni(OH)_2$	1M KOH + 0.33M Urea	14	1.46 V	[18]
$Mo_{0.05}$-Co-NiS/Ni_3S_4	1M KOH + 0.33M Urea	14	1.55 V	[19]
$NiFe_2O_4$/NF	1M KOH + 0.33M Urea	14	1.519 V	[20]

Table S3 Comparison of the HER performances of NiCoP-S and other reported electrocatalysts in alkaline seawater solution.

catalysts	Electrolytes	pH	Overpotential(V) at 100 mA/cm^2	Reference
NiCoP-S	**1M KOH+Seawater**	**13.6**	**139 mV**	**This work**
NiTe@FeOOH	1M KOH+Seawater	14	278 mV	[21]
S–$Fe(OH)_3$/NiSe/NF	1M KOH+Seawater	14	349 mV	[22]
CFM 0.3	1M KOH+0.5M NaCl	13.6	270 mV	[23]
NNNF@Mo_2N/FeO_xN_y	1M KOH+Seawater	13.82	142 mV	[24]
NiFe-LDH/Cu-IF	1M KOH+1M Na_2S	13.91	203 mV	[25]
MoS_2/S-CoP	1M KOH+Seawater	14	197 mV	[26]
B, V-Ni_2P	1M KOH+Seawater	14	162 mV	[27]
Cu_2O-CoO/CF	1M KOH+Seawater	14	295 mV	[28]
RuO_2-Ti_3C_2/NF	1M KOH+Seawater	14	156 mV	[29]
NiFe LDH-Ni_3S_2	1M KOH+Seawater	14	257 mV	[30]

Table S4 Comparison of solution diffusion resistance (Rs) and charge transfer resistance (Rct) values for all samples in alkaline solutions containing urea (HER).

catalyst	Rs(Ω)	Rct(Ω)
NiCoP-S	**1.651**	**0.894**
$Co(OH)_2$/NF	1.706	2.213
NiCoP	1.782	1.603
NiCoP-Se	1.609	1.127
NiCoP-N	1.583	0.943

Table S5 Comparison of solution diffusion resistance (Rs) and charge transfer resistance (Rct) values for all samples in alkaline solutions containing urea (UOR).

catalyst	Rs(Ω)	Rct(Ω)
NiCoP-S	**1.659**	**$6.738*10^{12}$**
$Co(OH)_2$/NF	1.683	$9.969*10^{15}$
NiCoP	1.88	$3.93*10^{15}$
NiCoP-Se	1.603	$4.027*10^{13}$
NiCoP-N	1.783	$4.59*10^{13}$

Table S6 Comparison of solution diffusion resistance (Rs) and charge transfer resistance (Rct) values for all samples in alkaline seawater solution (HER).

catalyst	Rs(Ω)	Rct(Ω)
NiCoP-S	**1.748**	**0.543**
$Co(OH)_2$/NF	1.773	1.257
NiCoP	1.781	0.979
NiCoP-Se	1.647	0.658
NiCoP-N	1.671	0.564

References

1. Hu, S.; Feng, C.; Wang, S.; Liu, J.; Wu, H.; Zhang, L.; Zhang, J., Ni_3N/NF as Bifunctional Catalysts for Both Hydrogen Generation and Urea Decomposition. *ACS Appl. Mater. Interfaces* **2019,** *11* (14), 13168-13175.
2. Guo, T.; Xu, X.; Wang, X.; Zhou, J.; Wang, H.; Shi, Z.; Huang, M., Enabling the full exposure of Fe_2P@Ni_xP heterostructures in tree-branch-like nanoarrays for promoted urea electrolysis at high current densities. *Chem. Eng. J.* **2021,** *417*, 128067.
3. Wang, C.; Lu, H.; Mao, Z.; Yan, C.; Shen, G.; Wang, X., Bimetal Schottky Heterojunction Boosting Energy-Saving Hydrogen Production from Alkaline Water via Urea Electrocatalysis. *Adv. Funct. Mater.* **2020,** *30* (21), 2000556.
4. Wen, D.; Ye, M.; Xia, Y.; Mai, W.; Zhang, Z.; Zhang, W.; Peng, W.; Hu, W.; Tian, L., CoP nanoplates dotted with porous Ni_3S_2 nanospheres for the collaborative enhancement of hydrogen production via urea-water electrolysis. *Appl. Surf. Sci.* **2022,** *586*, 152736.
5. Ding, Y.; Du, X.; Zhang, X., Rose-like Cu-doped Ni_3S_2 nanoflowers decorated with thin NiFe LDH nanosheets for high-efficiency overall water and urea electrolysis. *Appl. Surf. Sci.* **2022,** *584*, 152622.
6. Cao, J.; Li, H.; Zhu, R.; Ma, L.; Zhou, K.; Wei, Q.; Luo, F., Improved hydrogen generation via a urea-assisted method over 3D hierarchical NiMo-based composite microrod arrays. *J. Alloys Compd.* **2020,** *844*, 155382.
7. Lv, L.; Li, Z.; Wan, H.; Wang, C., Achieving low-energy consumption water-to-hydrogen conversion via urea electrolysis over a bifunctional electrode of hierarchical cuprous sulfide@nickel selenide nanoarrays. *J. Colloid Interface Sci.* **2021,** *592*, 13-21.

8. Zhao, Q.; Meng, C.; Kong, D.; Wang, Y.; Hu, H.; Chen, X.; Han, Y.; Chen, X.; Zhou, Y.; Lin, M.; Wu, M., In Situ Construction of Nickel Sulfide Nano-Heterostructures for Highly Efficient Overall Urea Electrolysis. *ACS Sustainable Chem. Eng.* **2021,** *9* (46), 15582-15590.
9. Huang, S.; Zhang, Q.; Xin, P.; Zhang, J.; Chen, Q.; Fu, J.; Jin, Z.; Wang, Q.; Hu, Z., Construction of Fe-doped NiS-NiS_2 Heterostructured Microspheres Via Etching Prussian Blue Analogues for Efficient Water-Urea Splitting. *Small* **2022,** *18* (14), 2106841.
10. Xiang, Y.; Yu, L.; Xiong, K.; Zhang, H.; Chen, J.; Shi, X.; Deng, M.; She, S., Nanoflowers $Ni(OH)_x$/p-Ni with in-situ formation of high-valence nickel for boosting energy-saving hydrogen production from urea-assisted water splitting. *Int. J. Hydrogen Energy* **2024,** *64*, 360-367.
11. Sha, L.; Yin, J.; Ye, K.; Wang, G.; Zhu, K.; Cheng, K.; Yan, J.; Wang, G.; Cao, D., The construction of self- supported thorny leaf- like nickel- cobalt bimetal phosphides as efficient bifunctional electrocatalysts for urea electrolysis. *J. Mater. Chem. A* **2019,** *7* (15), 9078-9085.
12. Wei, T.; Meng, G.; Zhou, Y.; Wang, Z.; Liu, Q.; Luo, J.; Liu, X., Amorphous Fe-Co oxide as an active and durable bifunctional catalyst for the urea-assisted H_2 evolution reaction in seawater. *Chem. Commun.* **2023,** *59* (66), 9992-9995.
13. Hao, J.; Li, J.; Zhu, Y.; Sun, S.; Lu, S.; Du, M.; Zhu, H., Ensemble effects of high entropy alloy for boosting alkaline water splitting coupled with urea oxidation. *Chem. Commun.* **2023,** *59* (6), 772-775.
14. Zheng, Y.; Tang, P.; Xu, X.; Sang, X., POM derived UOR and HER bifunctional NiS/MoS_2 composite for overall water splitting. *J. Solid State Chem.* **2020,** *292*, 121644.
15. Huang, C.-J.; Zhan, Q.-N.; Xu, H.-M.; Zhu, H.-R.; Shuai, T.-Y.; Li, G.-R., Fe-Doped Ni_2P/$NiSe_2$ Composite Catalysts for Urea Oxidation Reaction (UOR) for Energy-Saving Hydrogen Production by UOR-Assisted Water Splitting. *Inorg. Chem.* **2024,** *63* (19), 8925-8937.
16. Tong, R.; Xu, M.; Huang, H.; Wu, J.; Xiong, Y.; Shao, M.; Zhao, Y.; Wang, S.; Pan, H., Co_3Mo_3N nanosheets arrays on nickel foam as highly efficient bifunctional electrocatalysts for overall urea electrolysis. *Int. J. Hydrogen Energy* **2022,** *47* (22), 11447-11455.
17. Zhang, Y.; Guo, H.; Song, M.; Qiu, Z.; Wang, S.; Sun, L., Hierarchical interfaces engineering-driven of the CoS_2/MoS_2/Ni_3S_2/NF electrode for high-efficient and stable oxygen evolution and urea oxidation reactions. *Appl. Surf. Sci.* **2023,** *617*, 156621.
18. Miao, F.; Cui, P.; Gu, T.; Yu, S.; Yan, Z.; Hai, G., Dual cation-modified hierarchical nickel hydroxide nanosheet arrays as efficient and robust electrocatalysts for the urea oxidation reaction. *Dalton Trans.* **2024,** *53* (4), 1599-1606.
19. Huang, W.; Yuan, Y.; Wang, K.; Cao, Q.; Zhao, Y.; Sun, X.; Ding, R.; Gao, P.; Cai, W.; Liu, E., Tuning interface density and electronic structure of NiS/Ni_3S_4 by Mo, Co co-doping for efficient urea electrooxidation reaction. *J. Electroanal. Chem.* **2022,** *911*, 116242.
20. Yao, L.; Zhang, H.; Humayun, M.; Fu, Y.; Xu, X.; Feng, C.; Wang, C., Constructing nanoporous crystalline/amorphous $NiFe_2O_4$/NiO electrocatalyst for high efficiency OER/UOR. *J. Alloys Compd.* **2023,** *936*, 168206.
21. Gao, X.; Chen, J.; Yu, Y.; Wang, F.; Wu, X.; Wang, X.; Mao, W.; Li, J.; Huang, W.; Chen, Q.; Li, R.; You, C.; Wang, S.; Tian, X.; Kang, Z., Core-shell structured NiTe@FeOOH nanoarrays for efficient overall seawater splitting. *Chem. Eng. J.* **2023,** *474*, 145568.
22. Yang, C.; Jiang, X.; Li, Y.; Zeng, J.; Liang, H.-P., Construction of S-modified Amorphous $Fe(OH)_3$ on NiSe Nanowires as Bifunctional Electrocatalysts for Efficient Seawater Splitting. *ACS Appl. Nano Mater.* **2024,** *7* (4), 3960-3967.

23. Jin, S.; Liu, X.; Cao, J.; Wei, M.; Chen, Y.; Li, X.; Wu, Q.; Feng, B.; Han, M.; Jin, D.; Dong, Z.; Liu, X.; Liu, H., FeCo-MOF derived $Co_4S_3/Fe_3S_4/MoS_2$ nanosheet arrays on iron foam for overall water splitting in alkaline water /seawater at large-current density. *Int. J. Hydrogen Energy* **2024,** *61*, 329-340.

24. He, Y.; Hu, Y.; Zhu, Z.; Li, J.; Huang, Y.; Zhang, S.; Balogun, M. S.; Tong, Y., High-performance multidimensional-structured N-doped nickel modulated Mo_2N/FeO_xN_y bifunctional electrocatalysts for efficient alkaline seawater splitting. *Chem. Eng. J.* **2024,** *489*, 151348.

25. Jiang, J.; Tian, Y.; Zhang, J.; Zhang, C.; Ai, L., Metallic Cu-incorporated NiFe layered double hydroxide nanosheets enabling energy-saving hydrogen generation from chlorine-free seawater electrolysis coupled with sulfion upcycling. *Fuel* **2024,** *367*, 131506.

26. Li, X.; Wang, L.; Li, R.; Ke, M.; Zhou, Y.; Liu, J., Multi-dimensional MoS_2/S-doped-CoP heterostructure nanoarrays as an efficient electrocatalyst for hydrogen evolution reaction. *Ceram. Int.* **2024,** *50* (11), 18519-18527.

27. Zhao, T.; Wang, S.; Jia, C.; Rong, C.; Su, Z.; Dastafkan, K.; Zhang, Q.; Zhao, C., Cooperative Boron and Vanadium Doping of Nickel Phosphides for Hydrogen Evolution in Alkaline and Anion Exchange Membrane Water/Seawater Electrolyzers. *Small* **2023,** *19* (27), 2208076.

28. Xie, L.; Liu, Q.; He, X.; Luo, Y.; Zheng, D.; Sun, S.; Farouk, A.; Hamdy, M. S.; Liu, J.; Kong, Q.; Sun, X., A brush-like Cu_2O-CoO core-shell nanoarray: an efficient bifunctional electrocatalyst for overall seawater splitting. *Chem. Commun.* **2023,** *59* (68), 10303-10306.

29. Zhang, Y.; Zhang, Z.; Yu, Z.; Addad, A.; Wang, Q.; Roussel, P.; Szunerits, S.; Boukherroub, R., Ruthenium Oxide Nanoparticles Immobilized on Ti_3C_2 MXene Nanosheets for Boosting Seawater Electrolysis. *ACS Appl. Mater. Interfaces* **2023,** *15* (50), 58345-58355.

30. Zhang, Z.-H.; Yu, Z.-R.; Zhang, Y.; Barras, A.; Addad, A.; Roussel, P.; Tang, L.-C.; Naushad, M.; Szunerits, S.; Boukherroub, R., Construction of desert rose flower-shaped NiFe LDH-Ni_3S_2 heterostructures via seawater corrosion engineering for efficient water-urea splitting and seawater utilization. *J. Mater. Chem. A* **2023,** *11* (36), 19578-19590.